

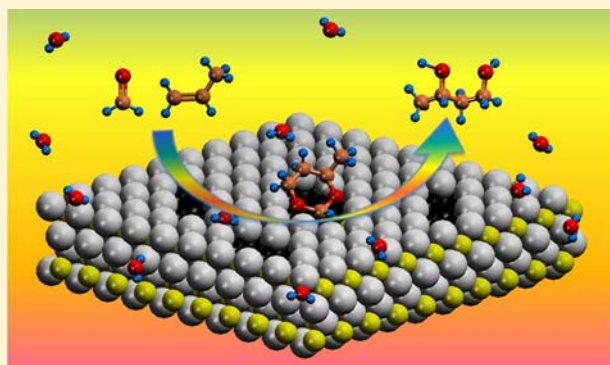
# Heterogeneous Ceria Catalyst with Water-Tolerant Lewis Acidic Sites for One-Pot Synthesis of 1,3-Diols via Prins Condensation and Hydrolysis Reactions

Yehong Wang, Feng Wang,\* Qi Song, Qin Xin, Shutao Xu, and Jie Xu\*

State Key Laboratory of Catalysis, Dalian National Laboratory for Clean Energy, Dalian Institute of Chemical Physics, Chinese Academy of Sciences, Dalian 116023, P. R. China

## S Supporting Information

**ABSTRACT:** The use of a heterogeneous Lewis acid catalyst, which is insoluble and easily separable during the reaction, is a promising option for hydrolysis reactions from both environmental and practical viewpoints. In this study, ceria showed excellent catalytic activity in the hydrolysis of 4-methyl-1,3-dioxane to 1,3-butanediol in 95% yield and in the one-pot synthesis of 1,3-butanediol from propylene and formaldehyde via Prins condensation and hydrolysis reactions in an overall yield of 60%. In-depth investigations revealed that ceria is a water-tolerant Lewis acid catalyst, which has seldom been reported previously. The ceria catalysts showed rather unusual high activity in hydrolysis, with a turnover number (TON) of 260, which is rather high for bulk oxide catalysts, whose TONs are usually less than 100. Our conclusion that ceria functions as a Lewis acid catalyst in hydrolysis reactions is firmly supported by thorough characterizations with IR and Raman spectroscopy, acidity measurements with IR and  $^{31}\text{P}$  magic-angle-spinning NMR spectroscopy,  $\text{Na}^+/\text{H}^+$  exchange tests, analyses using the in situ active-site capping method, and isotope-labeling studies. A relationship between surface vacancy sites and catalytic activity has been established.  $\text{CeO}_2(111)$  has been confirmed to be the catalytically active crystalline facet for hydrolysis. Water has been found to be associatively adsorbed on oxygen vacancy sites with medium strength, which does not lead to water dissociation to form stable hydroxides. This explains why the ceria catalyst is water-tolerant.



## INTRODUCTION

Unsupported crystalline bulk oxides characterized with high activity, selectivity, and stability, such as  $\text{MgO}$ , $^{1-6}$   $\text{VO}_x$ , $^{7,8}$   $\text{MoO}_3$ , $^{9-11}$   $\text{Fe}_2\text{O}_3$ , $^{12,13}$  and  $\text{Nb}_2\text{O}_5$ , $^{14}$  have been employed as catalysts in many organic transformations. Ceria ( $\text{CeO}_2$ ) and ceria-based materials have been used as active species, promoters, and/or supports of heterogeneous catalysts. The wide application of ceria is driven by its ability to store and release oxygen (by creating oxygen vacancy sites) because of the easily accessible redox cycle of cerium ions ( $\text{Ce}^{3+} \rightleftharpoons \text{Ce}^{4+}$ ) at reaction temperatures below 200 °C. $^{15,16}$  On the other hand, it is considered that under mild reaction conditions, surface oxygen is less mobile and firmly held in lattice matrix. Therefore, organic reactions taking place under these conditions may involve only the acid–base properties of ceria. $^{15}$

Hydrolysis reactions are greatly significant in both organic chemistry and industrial production, and are usually catalyzed by homogeneous or supported Brønsted acids in aqueous media. Homogeneous Lewis acid catalysts, such as  $\text{AlCl}_3$  and  $\text{BF}_3$ , decompose or are irreversibly deactivated in water. Generally, water is dissociatively adsorbed on Lewis acidic sites or oxygen vacancy sites of oxides to produce hydroxide and a proton, irreversibly reforming the oxide surface structure

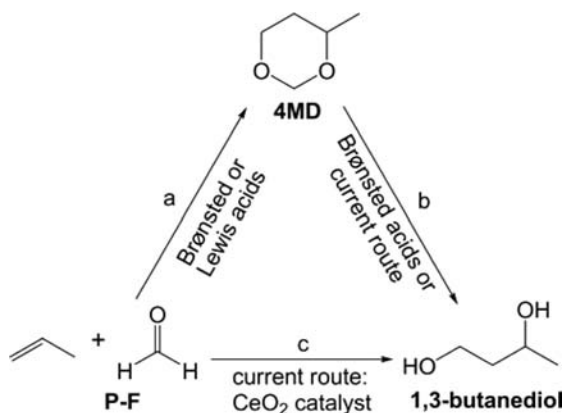
and leading to malfunction of the Lewis acidic sites. However, it has been found that  $\text{NbO}_4$  tetrahedra, $^{14}$  which are Lewis acidic sites on the  $\text{Nb}_2\text{O}_5 \cdot n\text{H}_2\text{O}$  surface, form  $\text{NbO}_4\text{--H}_2\text{O}$  adducts in the presence of water. Some of the adducts can still function as effective Lewis acidic sites for allylation and isomerization reactions in water. Corma and co-workers have reported a series of works on reactions in water catalyzed by Sn-based zeolites. $^{17-20}$  Their results show that Lewis acidic sites can practically be effective in water. Other examples, such as metal triflates, $^{21-28}$  metal chlorides, $^{29-32}$  and boron-based salts, $^{33-36}$  have also been claimed to be water-tolerant reusable catalysts, but none of them has been known to be catalytically active in hydrolysis reactions.

1,3-Butanediol is used as comonomer in some polyurethane and polyester resins, taking advantage of its good resistance, dyeability, and flexibility. $^{37,38}$  It can be prepared via acetaldehyde condensation and hydrogenation. $^{39}$  Propylene and formaldehyde (P-F), which are readily available starting materials, can be converted to 1,3-butanediol through a tandem reaction involving Prins condensation of P-F to 4-methyl-1,3-

Received: October 24, 2012

Published: December 10, 2012

dioxane (4MD) (Figure 1a) followed by hydrolysis of 4MD to 1,3-butanediol (Figure 1b). Prins condensations are known to



**Figure 1.** (a) Prins condensation of propylene and formaldehyde (P-F) to 4MD. (b) Hydrolysis of 4MD to 1,3-butanediol. (c) One-pot method reported here for the synthesis of 1,3-butanediol from P-F over a heterogeneous ceria catalyst.

be catalyzed by both homogeneous and heterogeneous Brønsted or Lewis acids.<sup>38</sup> Although the hydrolysis of substituted 1,3-dioxanes has been studied, only homogeneous or supported Brønsted acids have been reported to be active for the conversion.<sup>40,41</sup> The use of a heterogeneous Lewis acid catalyst, which is insoluble and easily separable from the reaction, is a promising option for this hydrolysis reaction from both environmental and practical viewpoints.

Here we report that ceria can highly efficiently catalyze the hydrolysis of 4MD to 1,3-butanediol in 95% yield (Figure 1b). This enabled us to realize the one-pot synthesis of 1,3-butanediol from P-F in up to 60% yield (Figure 1c). Detailed studies revealed that ceria is a water-tolerant Lewis acid catalyst that is resistant to water, recyclable, and reusable at least four times without loss of activity or selectivity. Since this catalytic behavior of ceria is rather unusual, we made a great effort to investigate the surface acidic nature of ceria. Our conclusions regarding the ceria catalyst are firmly based on the results of IR and Raman characterizations, acidity measurements with IR and <sup>31</sup>P magic-angle-spinning (MAS) NMR spectroscopy, Na<sup>+</sup>/H<sup>+</sup> exchange tests, analyses using the in situ active-site capping method, and isotope-labeling studies.

## EXPERIMENTAL SECTION

**Chemicals and Reagents.** All chemicals were of analytical grade and used as purchased without further purification. Most of chemicals were purchased from J&K Chemicals. (NH<sub>4</sub>)<sub>2</sub>[Ce(NO<sub>3</sub>)<sub>6</sub>] and Ce(NO<sub>3</sub>)<sub>3</sub>·6H<sub>2</sub>O were purchased from Aladdin Chemicals.

**Preparation of Ceria.** The ceria-A sample was obtained by calcination of (NH<sub>4</sub>)<sub>2</sub>[Ce(NO<sub>3</sub>)<sub>6</sub>] at 650 °C in air for 2 h, and ceria-B was provided by the Catalysis Society of Japan. The ceria-C sample was prepared by a conventional precipitation method. Briefly, 5.0 g of Ce(NO<sub>3</sub>)<sub>3</sub>·6H<sub>2</sub>O was dissolved in 100 mL of Millipore-purified water (18 mΩ·cm), and the solution was adjusted to pH 11.0 by the addition of NH<sub>4</sub>OH (3.4 M) under magnetic stirring at room temperature. The resulting gel mixture was washed with pure water, dried in an oven at 100 °C for 12 h, and calcined at 500 °C in air for 4 h.

**Preparation of Na<sup>+</sup>/Ceria-C, H<sup>+</sup>/Ceria-C, and Water-Treated CeO<sub>2</sub>.** The Na<sup>+</sup>/ceria-C sample was prepared using an ion-exchange method taken from the literature.<sup>14</sup> Typically, 2.0 g of ceria-C was added to 40 mL of a 1.0 M NaNO<sub>3</sub> solution. The suspended mixture was adjusted to pH 10 using 0.5 M NaOH solution. The mixture was

stirred for 1 h at 70 °C, and the solid was filtered out and washed with water until neutral (500 mL). The treatment was repeated three times to increase the ion-exchange level. Finally, the ion-exchanged sample was dried in an oven at 100 °C for 12 h. The H<sup>+</sup>/ceria-C sample was obtained by exchanging Na<sup>+</sup>/ceria-C with a 1.0 M NH<sub>4</sub>NO<sub>3</sub> solution (two exchanges at 70 °C for 1 h) followed by calcination at 500 °C for 4 h.<sup>42</sup> Water-treated CeO<sub>2</sub> was prepared by thermal treatment of a certain amount of fresh CeO<sub>2</sub> in an autoclave at 180 °C for 1 h. The sample was dried at 120 °C before using.

**Hydrolysis of 4-Methyl-1,3-dioxane.** Typically, 4MD (0.16 mL, 1.5 mmol), catalyst (0.1 g), water (1.0 mL), and a magnetic stir bar were loaded into a Teflon-lined autoclave reactor. The reactor was sealed and placed in a preheated red copper mantle at the desired temperature. Seven reactions could be conducted simultaneously in order to achieve parallel reaction conditions. Each reaction was continued for the desired time and then terminated by natural cooling to ambient temperature, after which samples were acquired for analysis. A 1% H<sub>2</sub>SO<sub>4</sub> solution (1 mL) was used as a catalyst. For comparison, 0.1 g of Sc(OTf)<sub>3</sub> with 1.5 mmol of sodium dodecyl sulfate (SDS) surfactant was used as catalyst.<sup>43</sup> The 4MD conversion and 1,3-butanediol selectivity were determined by normalizing the gas chromatography (GC) integration area since 4MD and 1,3-butanediol have similar coefficient factors in GC analysis. Product yields were calculated by multiplying the conversion by the selectivity.

**Kinetic Analysis of 4MD Hydrolysis.** Kinetic runs were carried out in the hydrolysis of 4MD at temperatures of 120, 130, 140, and 150 °C. The initial concentration of 4MD was 1.29 mol L<sup>-1</sup> in all reactions. The stirring speed was maintained at >350 rotations/min to eliminate mass transfer limitations.

**One-Pot Synthesis of 1,3-Butanediol.** Formaldehyde (38% formalin, 0.42 mL, 6.0 mmol of formaldehyde), catalyst (0.1 g), water (1.0 mL), and a magnetic stir bar were loaded into a Teflon-lined autoclave reactor. The reactor was then sealed and placed in a preheated red copper mantle at the desired temperature. Propylene (99.99%) was supplied from a cylinder and charged into the reactor to a pressure of 0.8 MPa. Products were analyzed by gas chromatography–mass spectrometry (GC–MS) using an Agilent 7890A/5975C instrument equipped with an HP-5MS column (30 m in length, 0.25 mm in diameter). Authenticated samples were used to quantify the reactants and products.

**Characterization by Diffuse-Reflectance IR Fourier Transform (DRIFT) Spectroscopy.** DRIFT spectra were collected on a Bruker Tensor 27 instrument to obtain information about surface hydroxyl groups. First, a powder sample was heated in situ in an IR cell (Harrick “Praying Mantis” diffuse reflectance accessory) at 180 °C in Ar (30 mL min<sup>-1</sup>). The sample was then cooled to 30 °C, and a background spectrum was recorded. After water adsorption for 10 min, the IR spectra for water desorption at different temperatures were also recorded. For data collection, the sample was cooled to 30 °C before the measurement.

**Characterization by Pyridine-Adsorption IR Analysis.** Quantification of acidity by the pyridine-adsorption IR method was conducted on a Bruker 70 IR spectrometer. The sample was pressed into a self-supporting disk (13 mm diameter, 25–27.7 mg) and placed in a homemade IR cell attached to a closed glass-circulation system. Prior to pyridine adsorption, the sample disk was pretreated by heating at 150 °C for 1 h in vacuum (pressure <10<sup>-3</sup> Pa) and then cooled to 30 °C. After a spectrum was collected, the sample disk was exposed to pyridine vapor. IR spectra of the chemisorbed pyridine were recorded after evacuation at 150 °C for 0.5 h (pressure <1.0 × 10<sup>-3</sup> Pa) to eliminate physically adsorbed pyridine. Spectra were collected after cooling to 30 °C. The calculation of the number of Lewis acidic sites was based on the following formula:<sup>44</sup>

$$C = 1.42 \times IA \times R^2/W$$

where  $C$  is the concentration [mmol (g of catalyst)<sup>-1</sup>],  $IA$  is the integrated absorbance of the L band (cm<sup>-1</sup>),  $R$  is the radius of the catalyst disk (cm), and  $W$  is the mass of the disk (mg).

**Coadsorption of Pyridine and Water and IR Characterization.** The coadsorption of pyridine with water was carried out on a

Thermo Scientific Nicolet iS10 FTIR spectrometer in absorbance mode. After adsorption of pyridine, water vapor (~1 Torr) was introduced into the IR cell. Spectra for adsorption of water for 1, 3, and 5 min at 30 °C were then collected.

**Acidity Measurement by  $^{31}\text{P}$  NMR Spectroscopy with Trimethylphosphine as a Probe Molecule.** A special device was designed to carry out the online treatment of samples.<sup>45</sup> In this apparatus, samples were dehydrated typically at 120 °C and at a pressure  $<10^{-3}$  Pa for 10 h before adsorption. After dehydration, 20 kPa trimethylphosphine (TMP) (Sigma-Aldrich) was introduced, and the system was kept for 30 min at room temperature and then degassed at 50 °C for 15 min to remove most of the physical adsorbates from the surface. Finally, the samples were placed in situ into an NMR rotor, sealed, and transferred to the spectrometer without exposure to air. Such handling of the samples avoided oxidation of TMP and also its toxicity.  $^{31}\text{P}$  MAS NMR spectra with high-power proton decoupling were recorded at room temperature on a Bruker Avance III 600 MHz spectrometer using a 4 mm MAS probe with a resonance frequency of 242.9 MHz. A total of 1024 scans were accumulated with a  $\pi/4$  pulse width of 1  $\mu\text{s}$  and a recycle delay of 4 s. Samples were spun at 12 kHz, and chemical shifts were referenced to 85%  $\text{H}_3\text{PO}_4$ . For the determination of quantitative results, all of the samples were weighed, and the spectra were calibrated by measurements on a known amount of  $(\text{NH}_4)_2\text{HPO}_4$  performed under the same conditions.

**Raman Characterization.** Raman spectra were recorded on a micro-Raman spectrometer (Renishaw) equipped with a CCD detector using a He/Ne laser with a wavelength of 514 nm.

## RESULTS AND DISCUSSION

**Catalyst Screening Tests and Optimization of the Reaction Conditions.** To achieve a one-pot synthesis of 1,3-butanediol, the priority was to develop a catalyst that could efficiently hydrolyze the diether bonds of 4MD (Figure 1b), which had not been previously reported over heterogeneous catalyst. We tested a variety of catalysts in the hydrolysis of 4MD in water (Figure 2). These catalysts have been tested in

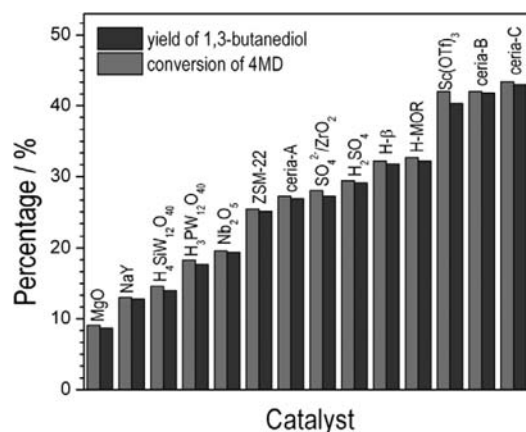


Figure 2. Catalyst screening tests in 4MD hydrolysis to 1,3-butanediol.

Prins condensation, but few of them have been employed in hydrolysis. Typical basic catalysts (MgO and NaY), Brønsted acids ( $\text{H}_4\text{SiW}_{12}\text{O}_{40}$ ,  $\text{H}_3\text{PW}_{12}\text{O}_{40}$ , H-β, and H-MOR), Lewis acids ( $\text{Nb}_2\text{O}_5$ , ZSM-22, and  $\text{SO}_4^{2-}/\text{ZrO}_2$ ), and mineral acids ( $\text{H}_2\text{SO}_4$ ) were active but afforded a 1,3-butanediol yield of less than ~30%. A 1,3-butanediol yield of 40% was achieved over a water-tolerant Lewis acid catalyst,  $\text{Sc}(\text{OTf})_3$ ,<sup>43</sup> indicating that the hydrolysis reaction can be catalyzed by a Lewis acid catalyst. Ceria-C gave the best result, a 43% yield of 1,3-butanediol, which is comparable to that with ceria-B (41%) and better than

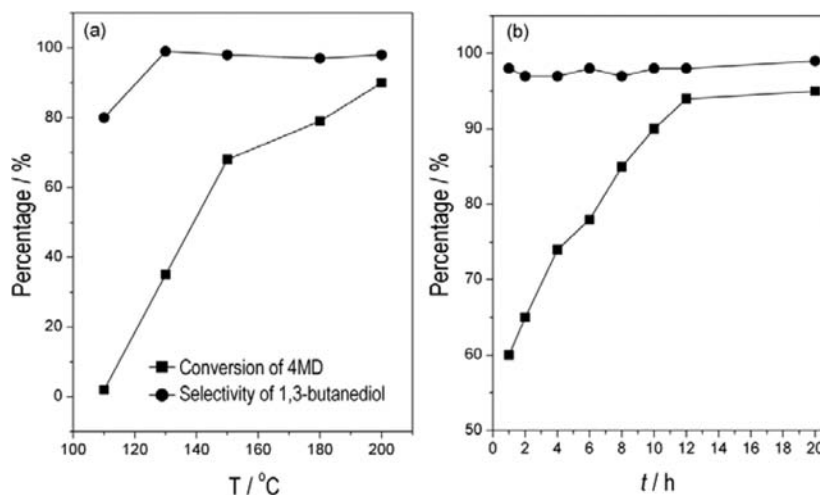
that with ceria-A (26%). These results indicate that ceria catalysts prepared by a particular method are more active and selective for 4MD hydrolysis than other catalysts under reaction conditions that need further optimization.

Optimization of the reaction conditions focused on the ceria-C catalyst in order to achieve a higher yield of 1,3-butanediol. Figure 3a shows the catalytic results at temperatures of 110–200 °C. The 4MD conversion increased rapidly from 2% at 110 °C to 68% at 150 °C and then to 90% at 200 °C. The 1,3-butanediol selectivity increased from 80% at 110 °C to 98% at 130 °C and then leveled off at 98% with a temperature increase to 200 °C. This behavior is typical for endothermic reactions. The reaction enthalpy ( $\Delta H$ ) at 25 °C was calculated to be 85  $\text{kJ}\cdot\text{mol}^{-1}$ . Further optimization of the reaction time was conducted at 180 °C (Figure 3b). The 1,3-butanediol selectivity was close to 99% throughout the course of the reaction. The 4MD conversion constantly increased to 94% after 12 h and leveled off at 95% after 20 h, suggesting that the hydrolysis equilibrium was established.

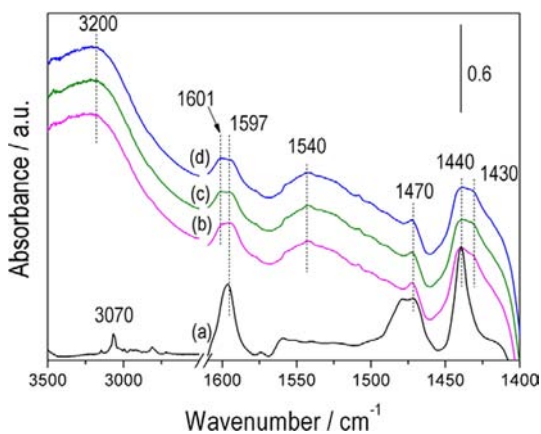
**Coadsorption of Pyridine with Water.** We employed pyridine-adsorption IR characterization to probe the surface acidity of ceria-C at 180 °C. The band at  $\sim 1540\text{ cm}^{-1}$ , which is usually assigned to Brønsted acidic sites, was not found in the spectrum of fresh  $\text{CeO}_2$  pretreated at 180 °C (Figure 4a). Two significant bands at 1440 and 1600  $\text{cm}^{-1}$  were observed, both attributed to coordinatively bound pyridine on Lewis acidic sites,<sup>46–50</sup> indicating that the ceria surface is predominantly covered by Lewis acidic sites. The band at 3070  $\text{cm}^{-1}$  is due to the C–H vibration of adsorbed pyridine. After adsorption of water on ceria for 1, 3, and 5 min (Figure 4b–d, respectively), the IR spectra changed. The band at 1440  $\text{cm}^{-1}$  broadened and shifted to lower wavenumber. A shoulder band at 1430  $\text{cm}^{-1}$  is assigned to a complex of water and pyridine. The band at 1470  $\text{cm}^{-1}$  can be assigned to hydrogen-bonded pyridine or coordinatively bonded pyridine. The weak, broad bands centered at 1540 and 1601  $\text{cm}^{-1}$  and the strong band centered at  $\sim 3200\text{ cm}^{-1}$  are probably due to physically adsorbed water. We thus conclude that in the presence of water, Lewis acidic sites are still present. The surface density of Lewis acidic sites was calculated to be 0.054  $\text{mmol g}^{-1}$  based on the band at 1440  $\text{cm}^{-1}$ .<sup>44</sup> The surface density of Ce cations was 0.883  $\text{mmol g}^{-1}$  based on the specific surface area of 67  $\text{m}^2\text{ g}^{-1}$  with the assumption of  $\text{CeO}_2(111)$  crystalline facets.<sup>47</sup> Therefore, it is roughly estimated that one out of every 16 Ce sites acts as a Lewis acidic site. The turnover number (TON) for ceria at 180 °C was 260, which is rather high for bulk oxide catalysts, whose TONs are usually less than 100, and much higher than the TON of 197 obtained over a  $\text{Nb}_2\text{O}_5\cdot n\text{H}_2\text{O}$  catalyst in the same reaction.

**Acidity Measured by Solid-State  $^{31}\text{P}$  MAS NMR Spectroscopy.** TMP has been employed to probe Brønsted and Lewis acidity in zeolites and other materials.<sup>51,52</sup> The interaction of TMP with bridging hydroxyl groups in zeolites leads to protonation of the probe molecules.  $^{31}\text{P}$  MAS NMR investigations have shown that the signal of protonated TMP occurs at –3 to –5 ppm, corresponding to the Brønsted acidic sites.<sup>51–53</sup> From Figure 5, the signals at –19.3 ppm can be ascribed to TMP adsorbed on Lewis acidic sites of the  $\text{CeO}_2$  and  $\text{Na}^+$ -exchanged  $\text{CeO}_2$  samples. No resonances in the range of –3 to –5 ppm due to interactions with Brønsted acid sites were observed. Quantification results showed that fresh  $\text{CeO}_2$  and  $\text{Na}^+$ -exchanged  $\text{CeO}_2$  had almost identical densities of Lewis acidic sites (0.065 and 0.063  $\text{mmol g}^{-1}$ , respectively),

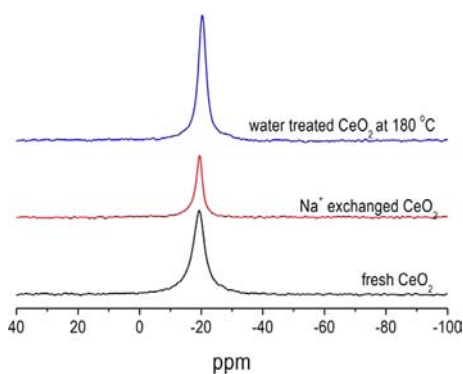




**Figure 3.** (a) Effect of reaction temperature on the catalytic performance of CeO<sub>2</sub> (ceria-C) in 4MD hydrolysis. (b) Time-on-stream profile at 180 °C.



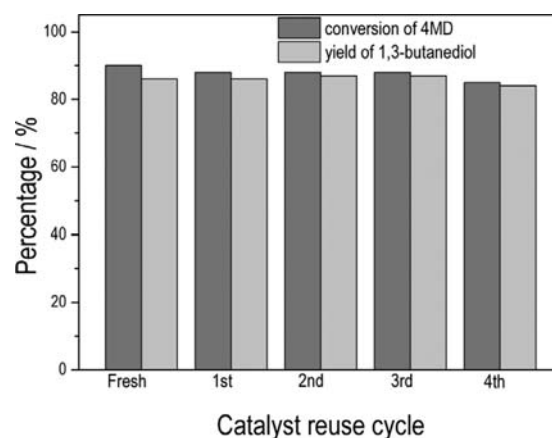
**Figure 4.** Pyridine-adsorption IR spectra of ceria-C at 180 °C (a) without and (b–d) with water adsorption for (b) 1, (c) 3, and (d) 5 min.



**Figure 5.** <sup>31</sup>P MAS NMR spectra of TMP adsorption on fresh, Na<sup>+</sup>-exchanged, and water-treated CeO<sub>2</sub> at 180 °C.

indicating that such ion-exchange treatment does not reform the surface Lewis acidity. This value is close to the value quantified by pyridine-adsorption IR spectroscopy (0.054 mmol g<sup>-1</sup>). We note that even a sample treated at 180 °C in water in an autoclave did not lose its Lewis acidity (0.065 mmol g<sup>-1</sup>), which clearly indicates that the Lewis acidity is water-tolerant. This is consistent with other characterization results provided in the following sections.

**Catalyst Stability.** The ceria catalyst could be filtered out from the reaction mixture and reused. The catalytic activities were comparable to those for the fresh catalyst after being recycled four times (Figure 6). This result indicates that ceria is

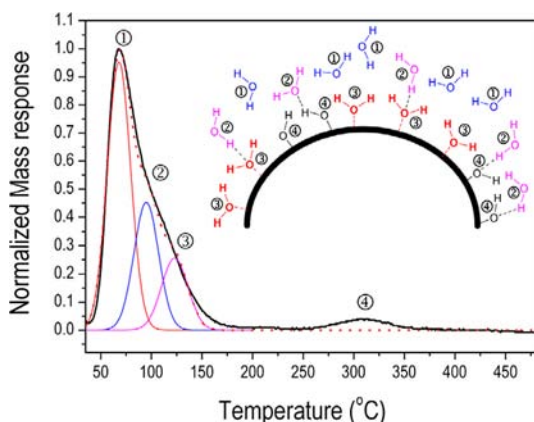


**Figure 6.** Reusability of ceria-C in the hydrolysis of 4MD to 1,3-butanediol.

a stable heterogeneous catalyst even in aqueous media. In many cases, however, water adsorption is an unavoidable process, since water is present as either a reactant or a spectator. The water–ceria interaction has been a heated topic of discussion because of its importance in understanding the catalytic behavior of ceria.<sup>54–58</sup> Coordinatively unsaturated surface Ce cation sites may cause water to be (i) associatively adsorbed as a proton and hydroxide with charge deviation or (ii) dissociated as a separated proton bound to a surface oxygen atom and hydroxide bound to cerium with charge transfer. Case (ii) is the common water–ceria interaction behavior under hydrothermal conditions at high temperature, which reforms ceria into a proton- and hydroxide-covered surface, resulting in the irreversible change in the surface acid–base properties. However, IR characterization of pyridine adsorption showed that ceria-C after water treatment at 180 °C followed by vacuum drying had nearly identical Lewis acidic sites as fresh ceria-C (Figure 4a,b), implying that the ceria–water interaction belongs to case (i), associative adsorption. In our reaction, the

water adsorption does not lead to reformation of the ceria surface, which leaves empty sites for adsorption of dioxane and formaldehyde.

It has been theoretically and experimentally shown that dissociatively adsorbed water is present on ceria (111) up to 300 °C.<sup>55,59</sup> This implies that water desorbing over the temperature interval 100–300 °C may belong to associatively adsorbed water on ceria. Temperature-programmed desorption (TPD) measurements are a convenient way of characterizing the water–ceria interaction.<sup>60,61</sup> An online analysis system equipped with a mass spectrometer was used to monitor the evolved gas (water, 18 amu). A profile of the 18 amu mass signal versus the temperature of sample is plotted in Figure 7.



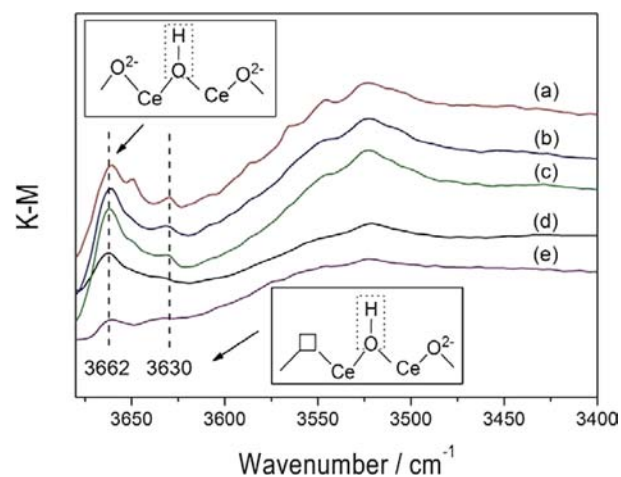
**Figure 7.** Profile of temperature-programmed desorption of water from ceria in flowing Ar gas (30 mL min<sup>-1</sup>). The numbers in circles indicate different adsorbed water species on ceria. The inset shows structures of the four types of surface water.

Two distinct peaks appear from 30 to 500 °C. To get more information on water adsorption, the experimental profile was fitted by a Lorentz function. The first peak contains three deconvoluted peaks with maxima at 68 °C (peak 1 in Figure 7), 96 °C (peak 2), and 122 °C (peak 3), corresponding to three types of water with overlapping desorption. Peak 1 is attributed to type-I water, which is included in the interparticle space and has no interaction with the ceria surface.<sup>62</sup> Peak 2 is due to type-II water, which interacts with surface-adsorbed water or hydroxide through hydrogen bonding. Peak 3 is ascribed to type-III water, which is associatively adsorbed on ceria. The second distinct peak with a maximum at 310 °C (peak 4 in Figure 7) is the result of dehydration of structural hydroxides, which has been explained previously.<sup>60,62</sup> In the hydrolysis reaction, only type-III water provides active protons needed for hydrolysis. The other three types of water are either molecularly adsorbed or dissociatively adsorbed without apparent acidity.

Following TPD tests, we measured the in situ IR spectra of samples calcined at 180, 200, 250, and 500 °C, respectively. The wide signals in the 3480–3600 cm<sup>-1</sup> range are ascribed to the surface residual cerium oxyhydroxide sites located within pores.<sup>63</sup> Some studies on silica reported this wavenumber range to correspond to geminal and triple hydroxyl groups.<sup>64</sup> The adsorption at 3662 cm<sup>-1</sup> is attributed to saturated surface hydroxyl groups, which are stable upon calcination at up to 500 °C. The peak at 3630 cm<sup>-1</sup> is due to surface hydroxyl groups neighboring oxygen vacancy sites.<sup>63</sup> In this study, the signal at 3630 cm<sup>-1</sup> was used as an indicator for the presence of oxygen

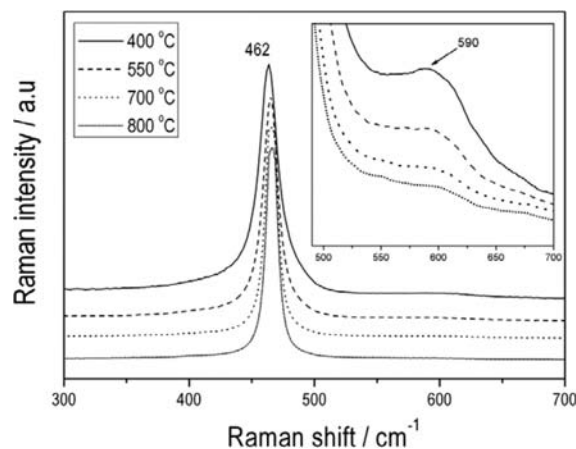
vacancy sites. It can be seen that these sites are stable in water at 180 °C, which is the real reaction condition, and can be oxidized upon an increase in calcination temperature. The combination of water-adsorption IR tests and TPD measurements showed that water adsorption on ceria is fairly weak, corresponding to associative adsorption under mild reaction conditions.

**Surface Oxygen Vacancy Sites and the Active Crystalline Facet.** In the ceria lattice, each oxygen anion is surrounded by a tetrahedron of cerium cations located at the center of a cubic arrangement of oxygen anions.<sup>65,66</sup> When ceria is heated at higher temperature in vacuum or under a reducing atmosphere, nonstoichiometric oxides CeO<sub>2-x</sub> (0 < x < 0.5), known as the Magneli phase, are usually obtained. As shown in Figure 8, calcination at elevated temperature oxidizes oxygen



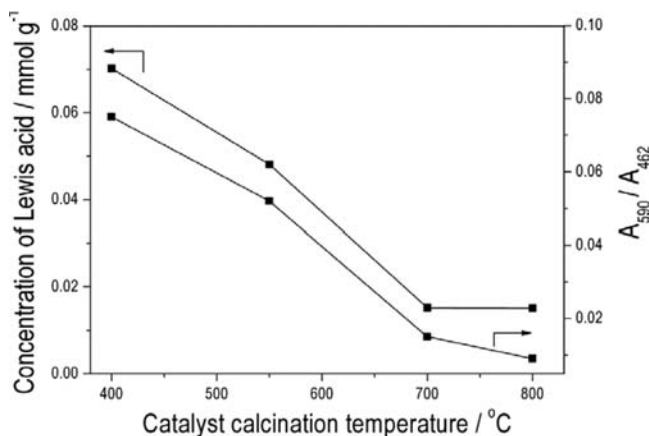
**Figure 8.** In situ FT-IR spectroscopic monitoring of water desorption (a–d) from ceria-C at (a) 180, (b) 200, (c) 250, and (d) 500 °C and (e) from ceria-C pretreated at 180 °C before water adsorption. The □ symbol indicates an oxygen vacancy site.

vacancies (decreasing *x* value) and accordingly decreases the Lewis acidity. Figure 9 shows the Raman shift of the calcined CeO<sub>2</sub> samples. Two bands were observed in all of the samples. The intense band at 460 cm<sup>-1</sup> is ascribed to the Raman-active F<sub>2g</sub> vibrational mode of the CeO<sub>2</sub> fluorite-type structure.<sup>67</sup> The weak band at 590 cm<sup>-1</sup> (Figure 9 inset) is associated with



**Figure 9.** Raman spectra (514 nm) of CeO<sub>2</sub> calcined at different temperatures in air.

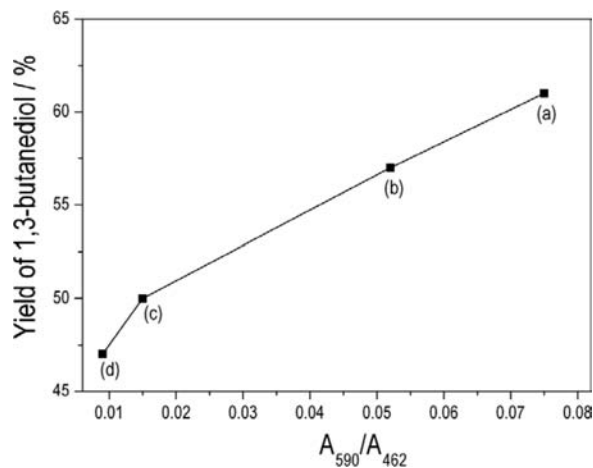
oxygen vacancy sites.<sup>68</sup> Because Raman spectroscopy with the 514 nm laser line provides only surface information for CeO<sub>2</sub>,<sup>69</sup> the oxygen vacancy sites detected by Raman spectroscopy predominantly exist on the CeO<sub>2</sub> surface. The ratio of the integrated peak areas under the bands at 590 and 462 cm<sup>-1</sup> ( $A_{590}/A_{462}$ ) can be used to quantify the relative surface concentration of oxygen vacancy sites.<sup>69,70</sup> The decrease in the  $A_{590}/A_{462}$  ratio with increasing calcination temperature indicates a gradual decrease in the number of surface oxygen vacancy sites and an overall decrease in the number of Lewis acidic sites (Figure 10). It is apparent that the concentration of



**Figure 10.** Dependence of surface concentration of oxygen vacancy sites and Lewis acidic sites of CeO<sub>2</sub> on calcination temperature.

surface oxygen vacancies measured by Raman scattering and the number of Lewis acidic sites obtained from pyridine-adsorption IR tests change in a similar way with increasing calcination temperature. A plot of the  $A_{590}/A_{462}$  ratio against the yield of 1,3-butanediol gives good linearity, indicating that oxygen vacancy sites of CeO<sub>2</sub> are catalytically active for 4MD hydrolysis to 1,3-butanediol (Figure 11).

It is known that the exposed crystalline facets of ceria, for example, the low-index crystalline facets (100), (110), and (111), have different surface concentrations of oxygen defect sites. Depending on the synthesis method, ceria with different exposed crystalline facets can be prepared, and they were



**Figure 11.** Plot of the yield of 1,3-butanediol versus the  $A_{590}/A_{462}$  ratio for samples calcined at (a) 400, (b) 550, (c) 700, and (d) 800 °C.

evaluated in this study to understand the active crystalline facet. On the basis of the reported methods,<sup>71,72</sup> we prepared uniform crystalline nanopolyhedra, nanorods, and nanocubes of CeO<sub>2</sub>. X-ray diffraction (XRD) and transmission electron microscopy (TEM) characterizations indicated that our results well-repeated those in the literature (Figures S4 and S5 in the Supporting Information). These samples selectively expose (111) and (100), (110) and (100), and (100) facets, respectively (Table 1). On the basis of theoretical calculations on surface oxygen vacancy sites of each crystalline phase,<sup>72</sup> we computed the total number of surface oxygen atoms (atoms nm<sup>-2</sup>) for each sample, which decreased in the sequence nanopolyhedron > nanocube > nanorod. Multiplying the total number of surface oxygen atoms by the specific surface area of each sample, we found that the number of surface oxygens per gram of ceria decreased in the sequence nanopolyhedron > nanorod > nanocube, which is exactly the same order as we obtained for the 1,3-butanediol yield in 4MD hydrolysis. We infer that the active crystalline facet for the hydrolysis reaction is the (111) facet, which is the most exposed facet for nanopolyhedral ceria (57% exposed on the basis of the data of Table 1). We note that the hydrolysis over ceria is less associated with its redox properties, which is a general consideration for high-temperature reactions (200–500 °C). However, our correlation of surface oxygen vacancy sites with 4MD hydrolysis is still meaningful because those sites of ceria are created upon calcination of the cerium precursor and remain intact during hydrolysis. The catalytic process mainly involves polarization of oxygen-containing bonds (water and dioxane) on vacancy sites (Ce<sup>3+</sup> sites). Our results agree well with previous studies that the ceria (111) crystalline facet is highly selective and active for organic reactions involving C–O or O–H bond activation under mild conditions.<sup>73–76</sup>

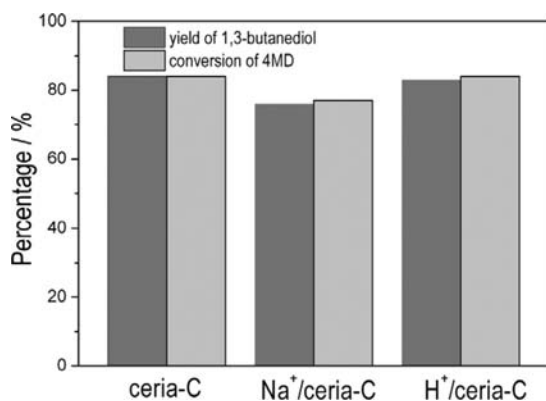
**Na<sup>+</sup>/H<sup>+</sup> Exchange.** Hydroxyl groups generated on the coordinatively unsaturated cations on surface of metal oxides are usually considered as Brønsted acidic sites when the materials are used in water.<sup>77</sup> The Na<sup>+</sup>/H<sup>+</sup> exchange method has been used to study the Lewis acidic sites of a niobic oxide catalyst.<sup>14</sup> We prepared two ceria samples to obtain a better understanding of the active sites of the ceria catalysts and to verify the reliability of the IR tests. One sample, Na<sup>+</sup>/ceria-C, was prepared by exchanging the possible surface Brønsted acidity of ceria-C with Na<sup>+</sup> to block Brønsted acidic sites, which was confirmed by pyridine-adsorption IR analysis (Figure S6 in the Supporting Information). The other sample, H<sup>+</sup>/ceria-C, was prepared by ion exchange of Na<sup>+</sup>/ceria-C with NH<sub>4</sub><sup>+</sup> followed by calcination to remove NH<sub>3</sub> and recover the surface acidity. The catalytic performances of ceria-C, Na<sup>+</sup>/ceria-C, and H<sup>+</sup>/ceria-C were compared under identical reaction conditions in the hydrolysis of 4MD, and the results are shown in Figure 12. The conversion of 4MD over Na<sup>+</sup>/ceria-C was slightly lower than with ceria-C, and the selectivity remained unchanged. H<sup>+</sup>/ceria-C catalyzed the reaction as well as ceria-C, indicating that the reactivity can be recovered by exchanging Na<sup>+</sup> with H<sup>+</sup>. This test again confirmed that the Lewis acidic sites of CeO<sub>2</sub> play a decisive role in catalyzing the hydrolysis of 4MD to 1,3-butanediol. Since 2003, Sato and co-workers have reported a series of works investigating why ceria stands out as an excellent catalyst among various oxides in the dehydration of diols (especially 1,3-butanediol) to unsaturated alcohols.<sup>78,79</sup> Experimental results and theoretical analysis have enabled them to conclude that surface oxygen vacancy sites play a key role in 1,3-butanediol activation. Although the hydrolysis reaction to



**Table 1.** Morphologies, Numbers of Surface Oxygen Atoms, and 1,3-Butanediol Yields over Different Types of Nanosized Ceria<sup>a</sup>

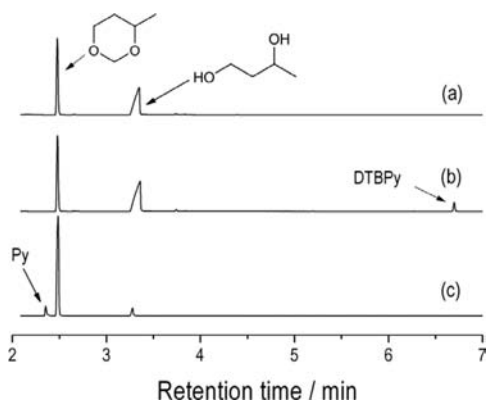
morphology	exposed crystalline facets and their ratio	total number of surface oxygen atoms (atoms nm <sup>-2</sup> )	S <sub>BET</sub> (m <sup>2</sup> g <sup>-1</sup> ) <sup>b</sup>	specific number of surface oxygen atoms (atoms g <sup>-1</sup> )	yield of 1,3-butanediol (%)
nanopolyhedron	(111):(100) = 8:6	(8/14) × 15.7 + (6/14) × 13.7 = 14.8	63	9.3 × 10 <sup>14</sup>	73
nanorod	(110):(100) = 4:2	(4/6) × 9.8 + (2/6) × 13.7 = 11.1	61	6.7 × 10 <sup>14</sup>	66
nanocube	(100) only	1 × 13.7 = 13.7	33	4.5 × 10 <sup>14</sup>	49

<sup>a</sup>Data of the theoretical exposed crystalline facets and their ratio and surface oxygen concentration are referenced from literature.<sup>72</sup> <sup>b</sup>Brunauer–Emmett–Teller (BET) surface area.

**Figure 12.** Results for hydrolysis of 4MD to 1,3-butanediol catalyzed by ceria-C, Na<sup>+</sup>/ceria-C, and H<sup>+</sup>/ceria-C.

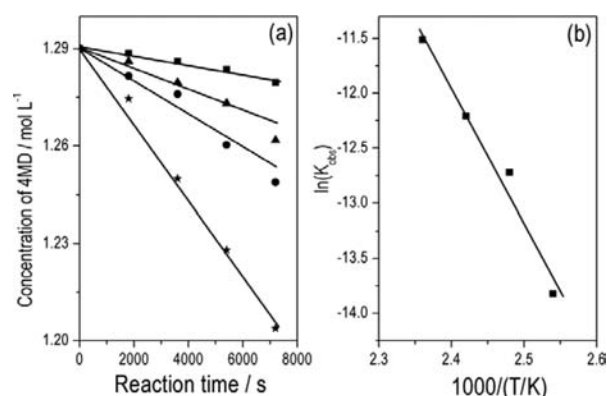
1,3-butanediol is obviously different from the dehydration reactions, we believe that at the molecular level, 1,3-butanediol may accommodate itself to an energetically favorable state on the ceria surface, which is beneficial for 1,3-butanediol in either its conversion or generation.<sup>80</sup>

**In Situ Capping Test.** Although pyridine-adsorption IR characterization did not show that ceria contains Brønsted acidic sites, the interaction with water during the reaction may generate hydroxyl moieties in the ceria if water is strongly adsorbed on oxygen vacancy sites. We employed pyridines for competitive adsorption with the reactants to probe the acidic character during the reaction.<sup>81,82</sup> Pyridine irreversibly reacts with Lewis and Brønsted acidic sites, while 2,6-di-*tert*-butylpyridine (DTBPy) selectively poisons Brønsted acid sites because of steric hindrance.<sup>17,83,84</sup> Through these tests, the catalytic nature (i.e., which acidic sites are active for catalysis) can be clearly disclosed. The 4MD hydrolysis was performed in the presence of pyridine or DTBPy (Figure 13). When DTBPy

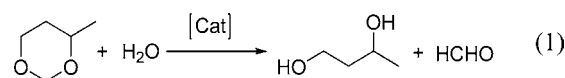
**Figure 13.** GC results for hydrolysis of 4MD to 1,3-butanediol (a) with no additive, (b) with 5% DTBPy, and (c) with 5% pyridine.

was present, the 1,3-butanediol yield was comparable to that for the reaction without DTBPy (52% in Figure 13b vs 51% in Figure 13a, respectively). In comparison, the use of pyridine remarkably suppressed the yield to 7% (Figure 13c). These results indicate that (i) the interaction of water with Ce cation sites does not block the Lewis acidity and (ii) Lewis acidic sites are accessible active sites for 4MD hydrolysis even in water. This reinforces our conclusion that ceria is a water-tolerant Lewis acid catalyst.

**Kinetic Analysis and Mechanism of Hydrolysis.** The reaction kinetics of the 4MD hydrolysis was studied at temperatures of 120–150 °C (Figure 14). The mass-transfer

**Figure 14.** (a) Kinetic analysis of the hydrolysis of 4MD at (■) 120, (▲) 130, (●) 140, and (★) 150 °C. (b) Arrhenius plot using the data in (a). The activation energy was found to be  $E_a = 103.1$  kJ·mol<sup>-1</sup>.

resistance was eliminated by increasing the speed of agitation until the reaction rate was not further increased. The 4MD hydrolysis reaction is shown in eq 1:



The concentrations of water and catalyst remained essentially constant during the reaction, allowing the dependence of the rate on 4MD to be isolated. Thus, the rate equation could be simplified as shown in eq 2:

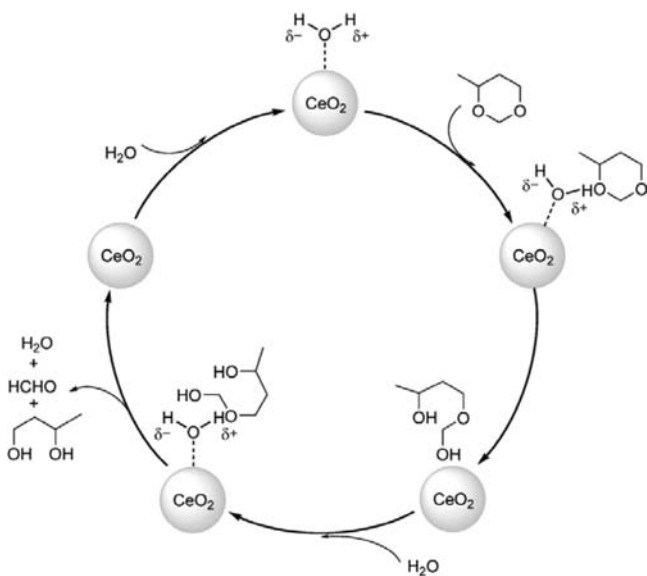
$$-\frac{d[4\text{MD}]}{dt} = k[\text{cat}]^\alpha [4\text{MD}]^\beta [\text{H}_2\text{O}]^\gamma = k_{\text{obs}}[4\text{MD}]^\beta \quad (2)$$

where [cat], [4MD], and [H<sub>2</sub>O] are the catalyst, 4MD, and water concentrations, respectively (mol L<sup>-1</sup>),  $k$  is the true reaction rate coefficient, and  $k_{\text{obs}}$  is the empirical pseudo- $\beta$ -order rate coefficient. The plot of [4MD] against time resulted in a linear relationship (Figure 14a), indicating a pseudo-zeroth-order reaction (i.e.,  $\beta = 0$ ). Thus, eq 2 could be further simplified to eq 3:

$$-\frac{d[4MD]}{dt} = k_{\text{obs}} \quad (3)$$

The  $k_{\text{obs}}$  values at 120, 130, 140, and 150 °C calculated from the slopes of the plots in Figure 14a were  $1.3 \times 10^{-6}$ ,  $3.5 \times 10^{-6}$ ,  $5.4 \times 10^{-6}$ , and  $1.2 \times 10^{-5}$  mol L<sup>-1</sup> s<sup>-1</sup>, respectively. A linear Arrhenius plot of  $\ln(k_{\text{obs}})$  versus  $1/T$  was obtained (Figure 14b), and the activation energy ( $E_a$ ) was calculated to be 103.1 kJ·mol<sup>-1</sup>.

A tentative reaction mechanism is thus proposed in Figure 15. Water is associately adsorbed on Lewis acidic sites of ceria,



**Figure 15.** Tentative reaction mechanism for hydrolysis of 4MD to 1,3-butanediol.

where it becomes polarized. Protonation of the secondary ether bond of 4MD leads to acetal formation and liberates the active site for next cycle. Another water molecule that has been activated on a Lewis acidic site then hydrolyzes the acetal to 1,3-butanediol, formaldehyde, and water, making an active site available for the next catalytic cycle. The proposed reaction mechanism is supported by isotope-labeling studies in which the hydrolysis was carried out in D<sub>2</sub>O instead of H<sub>2</sub>O. The molecular ion peak of 1,3-butanediol at  $m/z$  89 increased to  $m/z$  91 in for the reaction in D<sub>2</sub>O (the mass spectra are shown in

Figures S7 and S8 in the Supporting Information). This indicates that the two H atoms of the hydroxyls of 1,3-butanediol originate from water. The Ce sites on the surface act as Lewis acidic sites for substrate adsorption because they have an affinity for the oxygen atoms of dioxane and water, and they cause a polarization of the diether and H–OH bonds.<sup>47,73</sup> This proposal is well-supported by the control test in the presence of pyridine, which competitively adsorbs on Ce sites and thus blocks the initial substrate adsorption. A similar mechanism is known in the retro-Aldol reaction.<sup>85</sup> It is very possible that some specific surface anion sites or vacancy clusters on ceria may well accommodate 1,3-butanediol. Such a surface structure is beneficial for the production of 1,3-butanediol as well as for its dehydration at high temperature as reported by Ichikawa et al.<sup>80</sup>

**One-Pot Synthesis of 1,3-Butanediol.** We were further interested in the one-pot synthesis of 1,3-butanediol from P-F. Ceria-C catalyzed both the Prins condensation and 4MD hydrolysis and offered a 60% yield of 1,3-butanediol, which was the best result obtained in the study (Table 2). The other product was 4MD with 26% yield. The reactions over other basic (MgO) and acidic catalysts (H- $\beta$ , HY, heteropoly acids and SO<sub>4</sub><sup>2-</sup>/ZrO<sub>2</sub>) were sluggish and less selective toward 1,3-butanediol, either generating a great amount of tetrahydro-2H-pyran-4-ol and olefins or inefficiently catalyzing 4MD hydrolysis. The excellent performance of the ceria catalyst is attributed to its ability to catalyze the 4MD hydrolysis. To the best of our knowledge, this is the first report of the synthesis of 1,3-butanediol from P-F. We note that when a tandem reactor (one reactor for the Prins condensation and another downstream for the hydrolysis) was used in our study, the yield of 4MD in the first reactor reached 90% and the yield of 1,3-butanediol in the second reached 95%. The total yield of 1,3-butanediol reached 86%, which is better than that in a single reactor. This difference may be due to the following: (i) Lower temperature (<100 °C) is favorable for the Prins condensation. At the high temperature that is beneficial for hydrolysis (>160 °C), side reactions take place in the Prins condensation. (ii) Competitive activation of propylene, formaldehyde, and 4MD on catalytic sites may decrease the catalytic activity. In either case, the ceria catalyst plays a vital role for the 4MD hydrolysis.

The ceria catalyst was also tested in other hydrolysis reactions, including 1,3-dioxane and epoxides to diols and nitrile to amide (Table 3). 1,3-Dioxane was converted to 1,3-propanediol with 84% conversion and 86% selectivity in 24 h at

**Table 2. One-Pot Synthesis of 1,3-Butanediol from Propylene and Formaldehyde**

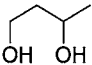
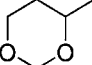
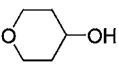
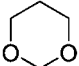

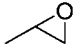
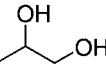
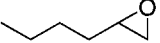
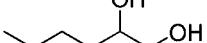
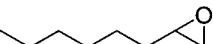
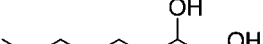
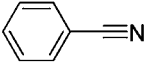
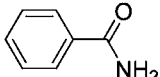
catalyst	yield/%			
				others
MgO	15	45	17	23
H- $\beta$	15	33	40	7
HY	18	45	27	5
H <sub>4</sub> SiW <sub>12</sub> O <sub>40</sub>	32	1	48	19
H <sub>3</sub> PW <sub>12</sub> O <sub>40</sub>	36	10	33	9
SO <sub>4</sub> <sup>2-</sup> /ZrO <sub>2</sub>	39	27	24	4
ceria-C	60	26	11	4



Table 3. Hydrolysis of Dioxane, Epoxides, and Benzonitrile over the Ceria Catalyst<sup>a</sup>

entry	substrate	product	T / °C	conv / %	sel / %
1 <sup>b</sup>			150	84	86
2 <sup>c</sup>			60	75	>99
3 <sup>d</sup>			100	>99	89
4 <sup>d</sup>			100	>99	96
5 <sup>e</sup>			150	44	>99

<sup>a</sup>The reaction time was 24 h. Products were determined by GC–MS. <sup>b</sup>1,3-Dioxane (1.5 mmol), H<sub>2</sub>O (1.0 mL), ceria-C (0.1 g). <sup>c</sup>Propylene oxide (1.0 mmol), H<sub>2</sub>O (1.0 mL), ceria-C (0.1 g). <sup>d</sup>Epoxide (1.5 mmol), H<sub>2</sub>O (10.0 mL), SDS (1.5 mmol), ceria-C (0.2 g). <sup>e</sup>Benzonitrile (1.5 mmol), H<sub>2</sub>O (1.0 mL), ceria-C (0.1 g).

150 °C (entry 1). Terminal epoxides with C3, C6, and C8 alkane chains were converted to the corresponding 1,2-diols in good to high yields (entries 2–4). C6 and C8 epoxides are immiscible in water, and therefore, SDS was needed as a surfactant. Hydrolysis of nitriles is a way to produce amides. As a representative reaction, benzonitrile was selectively converted to benzamide with >99% selectivity at moderate conversion of 44% (entry 5). All of these results indicate that the ceria catalyst can be used in various hydrolysis reactions.

## CONCLUSIONS

We have demonstrated that ceria is a highly active and selective catalyst in the hydrolysis of 4-methyl-1,3-dioxane to 1,3-butanediol in 95% yield. A high turnover number of 260 was observed, and the catalyst can be recycled and reused. Especially, ceria catalyzes the one-pot synthesis of 1,3-butanediol from propylene and formaldehyde in water via Prins condensation and 4-methyl-1,3-dioxane hydrolysis. We carefully investigated the nature of the ceria catalyst by spectroscopy and chemical adsorption methods. These characterization results clearly prove that ceria contains surface oxygen vacancy sites as Lewis acidic sites. The surface population of vacancy sites depends on the preparation method. A relationship between the surface oxygen vacancy sites and the catalytic activity was established. During the reaction, water is adsorbed on these sites with only medium strength and does not poison these sites, which explains why the ceria catalyst is stable in water. We believe that the present findings will open a new vista of ceria catalysts in aqueous reactions and greatly contribute to the understanding of other oxides as heterogeneous catalysts. Further mechanistic studies and applications to other reactions are underway.

## ASSOCIATED CONTENT

### Supporting Information

Catalyst preparation procedure and catalyst characterizations by XRD, N<sub>2</sub> adsorption, pyridine-adsorption IR spectroscopy, electron microscopy, and mass spectrometry. This material is available free of charge via the Internet at <http://pubs.acs.org>.

## AUTHOR INFORMATION

### Corresponding Author

wangfeng@dicp.ac.cn; xujie@dicp.ac.cn

### Notes

The authors declare no competing financial interest.

## ACKNOWLEDGMENTS

We sincerely thank Prof. Dr. Justin Notestein (Northwestern University) for help with preparation of the paper and valuable suggestions and comments. We thank Prof. Hongchen Guo and Dr. Cuilan Miao (State Key Laboratory of Fine Chemicals, Dalian University of Technology) for their generous help in IR tests. We also thank anonymous reviewers who gave valuable suggestions and comments that have helped to improve the quality of the manuscript. This work was supported by the National Natural Science Foundation of China (NNSFC) (Grants 21073184 and 21273231) and the One Hundred Person Project of the Chinese Academy of Sciences. S.X. acknowledges financial support from NNSFC (21103180).

## REFERENCES

- Pacchioni, G. *Chem. Phys. Solid Surf.* **2001**, *9*, 94.
- Cavani, F.; Maselli, L.; Passeri, S.; Lercher, J. A. *J. Catal.* **2010**, *269*, 340.
- Sheibani, H.; Amrollahi, M. A.; Esfandiarpour, Z. *Mol. Diversity* **2010**, *14*, 277.
- Selvamani, T.; Yagyu, T.; Kawasaki, S.; Mukhopadhyay, I. *Catal. Commun.* **2010**, *11*, 537.
- Reddy, M. B. M.; Ashoka, S.; Chandrappa, G. T.; Pasha, M. A. *Catal. Lett.* **2010**, *138*, 82.
- Kantam, M. L.; Mahendar, K.; Bhargava, S. *J. Chem. Sci.* **2010**, *122*, 63.
- Gao, X. H.; Lv, X. C.; Xu, J. *Kinet. Catal.* **2010**, *51*, 394.
- Chen, X.; Wang, F.; Xu, J. *Top. Catal.* **2011**, *54*, 1016.
- Wang, F.; Ueda, W.; Xu, J. *Angew. Chem., Int. Ed.* **2012**, *51*, 3883.
- Wang, F.; Ueda, W. *Chem.—Eur. J.* **2009**, *15*, 742.
- Wang, F.; Ueda, W. *Chem. Commun.* **2008**, 3196.
- Hermanek, M.; Zboril, R.; Medrik, I.; Pechousek, J.; Gregor, C. *J. Am. Chem. Soc.* **2007**, *129*, 10929.
- Zhu, J.; Ouyang, X.; Lee, M.-Y.; Davis, R. C.; Scott, S. L.; Fischer, A.; Thomas, A. *RSC Adv.* **2012**, *2*, 121.

- (14) Nakajima, K.; Baba, Y.; Noma, R.; Kitano, M.; Kondo, J. N.; Hayashi, S.; Hara, M. *J. Am. Chem. Soc.* **2011**, *133*, 4224.
- (15) Vivier, L.; Duprez, D. *ChemSusChem* **2010**, *3*, 654.
- (16) Murugan, B.; Ramaswamy, A. V. *J. Am. Chem. Soc.* **2007**, *129*, 3062.
- (17) Corma, A. *J. Catal.* **2000**, *191*, 218.
- (18) Corma, A. *J. Catal.* **2003**, *215*, 294.
- (19) Corma, A.; Navarro, M. T.; Renz, M. *J. Catal.* **2003**, *219*, 242.
- (20) Corma, A.; Renz, M. *Chem. Commun.* **2004**, 550.
- (21) Wiles, C.; Watts, P. *ChemSusChem* **2012**, *5*, 332.
- (22) Rebacz, N. A.; Savage, P. E. *Ind. Eng. Chem. Res.* **2010**, *49*, 535.
- (23) Kumar, A.; Rao, M. S.; Rao, V. K. *Aust. J. Chem.* **2010**, *63*, 135.
- (24) Aplander, K.; Ding, R.; Krasavin, M.; Lindstrom, U. M.; Wennerberg, J. *Eur. J. Org. Chem.* **2009**, 810.
- (25) Firouzabadi, H.; Iranpoor, N.; Farahi, S. *J. Mol. Catal. A: Chem.* **2008**, *289*, 61.
- (26) Prakash, G. K. S.; Yan, P.; Torok, B.; Bucsi, I.; Tanaka, M.; Olah, G. A. *Catal. Lett.* **2003**, *85*, 1.
- (27) Kobayashi, S. *Synlett* **1994**, 689.
- (28) Vergnaud, J.; Sarazin, Y.; Strub, H.; Carpentier, J. F. *Eur. Polym. J.* **2010**, *46*, 1093.
- (29) da Silva, M. L.; Figueiredo, A. P.; Cardoso, A. L.; Natalino, R.; da Silva, M. J. *J. Am. Oil Chem. Soc.* **2011**, *88*, 1431.
- (30) Goncalves, C. E.; Laier, L. O.; da Silva, M. J. *Catal. Lett.* **2011**, *141*, 1111.
- (31) Firouzabadi, H.; Iranpoor, N.; Jafarpour, M.; Ghaderi, A. *J. Mol. Catal. A: Chem.* **2006**, *252*, 150.
- (32) Bartoli, G.; Marcantoni, E.; Sambri, L. *Synlett* **2003**, 2101.
- (33) Longuet, C.; Joly-Duhamel, C.; Ganachaud, F. *Macromol. Chem. Phys.* **2007**, *208*, 1883.
- (34) Ishihara, K.; Yamamoto, H. *Eur. J. Org. Chem.* **1999**, 527.
- (35) Futatsugi, K.; Yamamoto, H. *Angew. Chem., Int. Ed.* **2005**, *44*, 1484.
- (36) Ishihara, K.; Hanaki, N.; Funahashi, M.; Miyata, M.; Yamamoto, H. *Bull. Chem. Soc. Jpn.* **1995**, *68*, 1721.
- (37) Sugiura, M.; Hayakawa, R. *Contact Dermatitis* **1997**, *1997*, 6.
- (38) Arundale, E.; Mikeska, L. A. *Chem. Rev.* **1952**, *51*, 505.
- (39) Shimizu, Y.; Sugimoto, S. i.; Kawanishi, S.; Suzuk, N. *Chem. Lett.* **1991**, 2.
- (40) Green, T. W.; Wuts, P. G. M. *Protective Groups in Organic Synthesis*; Wiley-Interscience: New York, 1999.
- (41) Qi, Y.; Xu, X.; Li, N.; Fang, Y. *Sep. Sci. Technol.* **2011**, *47*, 584.
- (42) Jobic, H.; Tuel, A.; Krossner, M.; Sauer, J. *J. Phys. Chem.* **1996**, *100*, 19545.
- (43) Kobayashi, S.; Manabe, K. *Acc. Chem. Res.* **2002**, *35*, 209.
- (44) Emeis, C. A. *J. Catal.* **1993**, *141*, 347.
- (45) Zhang, W.; Xu, S.; Han, X.; Bao, X. *Chem. Soc. Rev.* **2012**, *41*, 192.
- (46) Parry, E. P. *J. Catal.* **1963**, *2*, 371.
- (47) Tamura, M.; Wakasugi, H.; Shimizu, K.; Satsuma, A. *Chem.—Eur. J.* **2011**, *17*, 11428.
- (48) Yang, N. C.; Yang, D. D. H.; Ross, C. B. *J. Am. Chem. Soc.* **1959**, *81*, 133.
- (49) Sasikala, R.; Shirole, A. R.; Sudarsan, V.; Kamble, V. S.; Sudakar, C.; Naik, R.; Rao, R.; Bharadwaj, S. R. *Appl. Catal., A* **2010**, *390*, 245.
- (50) Tamura, M.; Shimizu, K.; Satsuma, A. *Appl. Catal., A* **2012**, *433*, 135.
- (51) Lunsford, J. H.; Rothwell, W. P.; Shen, W. *J. Am. Chem. Soc.* **1985**, *107*, 1540.
- (52) Kao, H. M.; Grey, C. P. *J. Am. Chem. Soc.* **1997**, *119*, 627.
- (53) Chu, Y.; Yu, Z.; Zheng, A.; Fang, H.; Zhang, H.; Huang, S.-J.; Liu, S.-B.; Deng, F. *J. Phys. Chem. C* **2011**, *115*, 7660.
- (54) Molinari, M.; Parker, S. C.; Sayle, D. C.; Islam, M. S. *J. Phys. Chem. C* **2012**, *116*, 7073.
- (55) Matolin, V.; Matolinova, I.; Dvorak, F.; Johaneck, V.; Myslivecek, J.; Prince, K. C.; Skala, T.; Stetsovych, O.; Tsud, N.; Vaclavu, M.; Smid, B. *Catal. Today* **2012**, *181*, 124.
- (56) Kinch, R. T.; Cabrera, C. R.; Ishikawa, Y. *J. Phys. Chem. C* **2009**, *113*, 9239.
- (57) Yang, Z. X.; Wang, Q. G.; Wei, S. Y. *Phys. Chem. Chem. Phys.* **2011**, *13*, 9363.
- (58) Fronzi, M.; Piccinin, S.; Delley, B.; Traversa, E.; Stampfl, C. *Phys. Chem. Chem. Phys.* **2009**, *11*, 9188.
- (59) Yang, Z. X.; Wang, Q. G.; Wei, S. Y.; Ma, D. W.; Sun, Q. A. *J. Phys. Chem. C* **2010**, *114*, 14891.
- (60) Bernal, S.; Calvino, J. J.; Cifredo, G. A.; Gatica, J. M.; Omil, J. A. P.; Pintado, J. M. *J. Chem. Soc., Faraday Trans.* **1993**, *89*, 3499.
- (61) Schoiswohl, J.; Tzvetkov, G.; Pfuner, F.; Ramsey, M. G.; Surnev, S.; Netzer, F. P. *Phys. Chem. Chem. Phys.* **2006**, *8*, 1614.
- (62) Gun'ko, V. M.; Zarko, V. I.; Chuikov, B. A.; Dudnik, V. V.; Ptushinskii, Y. G.; Voronin, E. F.; Pakhlov, E. M.; Chuiko, A. A. *Int. J. Mass Spectrom. Ion Processes* **1998**, *172*, 161.
- (63) Badri, A.; Binet, C.; Lavalley, J. C. *J. Chem. Soc., Faraday Trans.* **1996**, *92*, 4669.
- (64) Takeji, T.; Kato, K.; Meguro, A.; Chikazawa, M. *Colloids Surf., A* **1999**, *150*, 77.
- (65) Binet, C.; Daturi, M.; Lavalley, J. C. *Catal. Today* **1999**, *50*, 207.
- (66) Ganduglia-Pirovano, M. V.; Hofmann, A.; Sauer, J. *Surf. Sci. Rep.* **2007**, *62*, 219.
- (67) Shyu, J. Z.; Weber, W. H.; Gandhi, H. S. *J. Phys. Chem.* **1988**, *92*, 6.
- (68) Popović, Z. V.; Dohčević-Mitrović, Z.; Konstantinović, M. J.; Šćepanović, M. *J. Raman Spectrosc.* **2007**, *38*, 750.
- (69) Pu, Z.-Y.; Lu, J.-Q.; Luo, M.-F.; Xie, Y.-L. *J. Phys. Chem. C* **2007**, *111*, 18695.
- (70) Meng, L.; Jia, A.-P.; Lu, J.-Q.; Luo, L.-F.; Huang, W.-X.; Luo, M.-F. *J. Phys. Chem. C* **2011**, *115*, 19789.
- (71) Yang, S. W.; Gao, L. *J. Am. Chem. Soc.* **2006**, *128*, 9330.
- (72) Mai, H. X.; Sun, L. D.; Zhang, Y. W.; Si, R.; Feng, W.; Zhang, H. P.; Liu, H. C.; Yan, C. H. *J. Phys. Chem. B* **2005**, *109*, 24380.
- (73) Laursen, S.; Combita, D.; Hungria, A. B.; Boronat, M.; Corma, A. *Angew. Chem., Int. Ed.* **2012**, *51*, 4190.
- (74) Wang, X. W.; Zhao, G. M.; Zou, H. B.; Cao, Y. J.; Zhang, Y. G.; Zhang, R. B.; Zhang, F.; Xian, M. *Green Chem.* **2011**, *13*, 2690.
- (75) Badri, A.; Binet, C.; Lavalley, J. C. *J. Chem. Soc., Faraday Trans.* **1996**, *92*, 1603.
- (76) Tamura, M.; Tonomura, T.; Shimizu, K.-i.; Satsuma, A. *Green Chem.* **2012**, *14*, 717.
- (77) Zaki, M. I.; Hasan, M. A.; Al-Sagheer, F. A.; Pasupulety, L. *Colloids Surf., A* **2001**, *190*, 261.
- (78) Sato, S.; Takahashi, R.; Sodesawa, T.; Honda, N.; Shimizu, H. *Catal. Commun.* **2003**, *4*, 77.
- (79) Sato, F.; Okazaki, H.; Sato, S. *Appl. Catal., A* **2012**, *419*, 41.
- (80) Ichikawa, N.; Sato, S.; Takahashi, R.; Sodesawa, T. *J. Mol. Catal. A: Chem.* **2005**, *231*, 181.
- (81) Wang, F.; Ueda, W. *Top. Catal.* **2008**, *50*, 90.
- (82) Wang, F.; Xu, J.; Liao, S. *J. Chem. Commun.* **2002**, 626.
- (83) Marczewski, M.; Migda, A.; Marczevska, H. *Phys. Chem. Chem. Phys.* **2003**, *5*, 423.
- (84) Corma, A.; Fornés, V.; Forni, L.; Márquez, F.; Martínez-Triguero, J.; Moscotti, D. *J. Catal.* **1998**, *179*, 8.
- (85) Carey, F. A. *Organic Chemistry*, 4th ed.; McGraw-Hill, 2000; p 1002.

## NOTE ADDED AFTER ASAP PUBLICATION

This paper was published ASAP on January 11, 2013, with an error in the units of  $k_{\text{obs}}$  in the text following eq 3. The corrected version was reposted on January 14, 2013.